Peptide–Oleate Complexes Create Novel Membrane-Bound Compartments

Jesper S Hansen,[†,1,2] Tuan Hiep Tran,[†,1] Michele Cavalera,[1] Sanchari Paul,[1] Arunima Chaudhuri,[1] Karin Lindkvist-Petersson,[2] James C S Ho,[1,3] and Catharina Svanborg[*,1]

[1]Department of Microbiology, Immunology and Glycobiology, Institute of Laboratory Medicine, Lund University, Lund, Sweden

[2]Experimental Medical Science, Medical Structural Biology, Lund University, Lund, Sweden

[3]Centre for Biomimetic Sensor Science, School of Materials Science and Engineering, Nanyang Technological University, Singapore, Singapore

[†]These authors contributed equally to this work.

[*]**Corresponding author**: E-mail: catharina.svanborg@med.lu.se.

Associate editor: Banu Ozkan

Abstract

A challenging question in evolutionary theory is the origin of cell division and plausible molecular mechanisms involved. Here, we made the surprising observation that complexes formed by short alpha-helical peptides and oleic acid can create multiple membrane-enclosed spaces from a single lipid vesicle. The findings suggest that such complexes may contain the molecular information necessary to initiate and sustain this process. Based on these observations, we propose a new molecular model to understand protocell division.

Key words: **cell division, protocells, giant unilamellar vesicles, oleic acid, peptides, peptide–oleate complexes, phospholipids.**

Introduction

Membrane compartments are essential to create functional diversity in living organisms. The beginning of life necessitated such confinements to entrap macromolecules involved in simple biochemical reactions, creating early life protocells (Murtas 2013). According to a widely accepted evolutionary model, early protocell membranes consisted purely of fatty acids like oleic acid (Schrum et al. 2010; Lancet et al. 2018). Formed by self-assembly, the protocells have been shown to emerge when a critical aggregation concentration is reached and division of oleic acid membranes has been explained by a combination of thermal and mechanical forces (Budin et al. 2009).

Fatty acid membranes are thought to have evolved through an intermediate fatty acid/phospholipid hybrid state to phospholipid bilayer-enclosed entities that resemble cells (Schrum et al. 2010; Exterkate et al. 2018). The evolution of the oleic acid protocell likely began by incorporation of new constituents with a more complex acyl-chain repertoire, for instance longer-chain fatty acids (Budin et al. 2014). Vesicle growth is most often demonstrated experimentally by feeding existing vesicles with oleic acid. Intriguingly, the incorporation of dipeptide catalysts, which presumably existed prebiotically, also enhances vesicle growth (Adamala and Szostak 2013). Further, vesicle growth is promoted by environmental chemicals like thiols, polyelectrolytes, adenosine triphosphate, polynucleotides, or photoactive compounds (Zhu et al. 2012; Tang et al. 2014).

Protocell division, which is recognized as an essential first step in the evolution of higher organisms, is not readily induced under these conditions, however. Although oleic acid membranes may undergo tubulation and shearing-induced division, conditions that define the evolution of stable, multilumen vesicles still remain elusive (Budin et al. 2012). In this study, we observed dramatic and unexpected membrane effects of peptide–oleate complexes derived from α-lactalbumin; a homolog of lysozyme, which is produced by viruses, bacteria, fungi, and plants, and is present in various tissues and fluids of birds and mammals (Prager and Wilson 1988; Aminlari et al. 2014). Alpha-lactalbumin is structurally flexible (Mok et al. 2005), and transitions from the native folded state to a partially unfolded state form stable protein-fatty acid complexes that trigger extensive plasma membrane remodeling in tumor cells (Nadeem et al. 2015).

Here, we sought to investigate the membrane effects of peptides derived from α-lactalbumin and discovered that these peptides form peptide–oleate complexes that create multivesicular entities from single giant unilamellar vesicles (GUVs). The C-terminal, alpha-helical peptide showed the most pronounced membrane effect. After polar membrane elongation, a waist formed, followed by division into two or several large membrane-enclosed spaces. The results suggest a model to understand how fatty acid/phospholipid

intermediates can divide, aided only by a small peptide capable of binding oleic acid. We speculate that division can be achieved by this very simple system, a system simpler than any that has shown division before.

Results

Peptide–Oleate Complexes Trigger Formation of Multiple Membrane-Enclosed Entities from Single Protocells

Here, we tested the hypothesis that certain peptide–oleate complexes may create multiple, membrane-enclosed entities from single protocells. We obtained synthetic peptides comprising the N-terminal α-helical domain of human α-lactalbumin (alpha1, residues 1–39), the beta-sheet domain (beta, residues 40–80), or the C-terminal α-helical domain (alpha2, residues 81–123). The alpha-helical peptides formed complexes with deprotonated oleic acid, with an approximate stoichiometry of four oleate molecules per peptide (Ho et al. 2013). The alpha1 and alpha2 peptides are conformationally fluid but retain significant alpha-helical structure when bound to oleate (Brisuda A, Ho J, Kandiyal P, Ng J, Ambite I, Butler D, Háček J, Tran TH, Wan MLY, Hastings A, Tran TH, Fortunati D, Storm P, Nadeem A, Novotna H, Horňák J, Hansen JS, Mu YG, Mok KH, Babjuk M, Svanborg C, unpublished data).

GUVs were prepared from rhodamine-labeled egg phosphatidyl choline, which consists of 16- and 18-carbon saturated and monounsaturated lipid species and to a smaller extent of 18- and 20-carbon polyunsaturated lipid species. These carbonyl chain lengths are the predominant species in nature and therefore biologically relevant (Spector and Yorek 1985). GUVs were made by the hydrogel-assisted swelling method in an osmotically balanced 200 mM monosaccharide solution in phosphate-buffered saline (Horger et al. 2009; Hansen et al. 2013) and exposed to the peptide–oleate complexes. Changes in GUV morphology were monitored, by real-time confocal imaging (fig. 1).

Alpha2-oleate (21 μM) showed the most pronounced effect. After polar membrane elongation, a "waist" was formed, followed by division into two or several micrometer-sized membrane-enclosed spaces (8/20 GUVs, 40%, $P < 0.0001$ compared with untreated GUVs, fig. 1A and supplementary table 3 and supplementary video 1, Supplementary Material online). With time, the vesicle boundaries became more tense and the spherical daughter vesicles eventually existed as separate entities, indicating vesicle division. In some cases, the peptide–oleate complex created multiple interconnected membrane-enclosed spaces, which remained largely spherical, sometimes connected to the mother vesicle by a narrow membrane neck. In the remaining GUVs exposed to alpha2-oleate, smaller membrane vesicles and blebs were formed, suggesting a total GUV response rate of 100% (supplementary table 3, Supplementary Material online). Some of the blebs were subsequently pinched off when the neck regions were contracted.

Like alpha2-oleate, alpha1-oleate triggered vesicle division, but less frequently (2/13 GUVs). In the majority of GUVs, alpha1-oleate (21 μM) triggered formation of micron-sized nonsymmetrical membrane vesicles (13/13 GUVs, 100%, $P = 0.0001$ compared with untreated GUVs, fig. 1B and supplementary table 3 and supplementary video 2, Supplementary Material online). The vesicles were of nonuniform sizes and some were subsequently pinched off when the neck regions were contracted. Smaller membrane blebs were also formed at different time points, suggesting a diverse membrane response.

The beta-oleate complex did not create membrane protrusions and the naked alpha1 or alpha2 peptides were largely inactive (fig. 1C and supplementary video 3, Supplementary Material online). Oleic acid alone expectedly partitioned into lipid bilayers as evidenced by focal membrane thickening and some degree of internal membrane tubulation (Nadeem et al. 2015). Control GUVs in osmotically balanced glucose solution did not significantly change morphology over the experimental period (fig. 1C).

The results suggest that oleate complexes formed by alpha1 and alpha2 peptides from alpha-lactalbumin drive the formation of novel membrane-enclosed entities from a single GUV.

Peptide–Oleate Complexes Become Integrated into Vesicle Membranes

Membrane integration of the peptide–oleate complexes was confirmed by confocal imaging, using Alexa Fluor 488 (Alexa 488)-labeled alpha1- and alpha2-oleate and Alexa Fluor 633 (Alexa 633)-beta-oleate complexes (fig. 2A, B, and D). Strong colocalization with the membrane rhodamine marker was observed already after 3–5 min. The membrane signal was quantified by the analytical software of the LSM 510 microscope, showing significant colocalization of alpha1-oleate and alpha2-oleate with rhodamine (fig. 2C).

Membrane integration of the beta-oleate complexes was suggested by colocalization with the rhodamine marker, but without detectable alterations of the GUV morphology (fig. 2D). Membrane integration of the Alexa 488-alpha1, Alexa 488-alpha2, and Alexa 633-beta peptides was detected by confocal imaging, as colocalization with the rhodamine marker (fig. 2).

The results suggest that the N- or C-terminal α-helical domains of α-lactalbumin have affinity for lipid bilayers and that oleate complexes formed by these peptides become integrated into the lipid bilayer of the GUVs.

Encapsulated Macromolecular Payloads Are Propagated from Parent to Offspring Vesicles

Solute encapsulation in GUVs is often used to address if macromolecular cargo is propagated to daughter vesicles when the mother GUV forms new, membrane-enclosed entities (Helfrich et al. 2002; Dominak and Keating 2007; Fanti et al. 2018). To address this question, fluorescein isothiocyanate (FITC)-dextran (4 kDa) was incorporated into the GUVs and changes in membrane structure and cargo distribution were followed by live-cell imaging (fig. 3). After exposure to alpha2-oleate (21 μM), 7/20 GUVs underwent division and in all, FITC-dextran was efficiently propagated into the offspring GUVs (fig. 3A and supplementary video 4 and supplementary table 4, Supplementary Material online). In addition, another

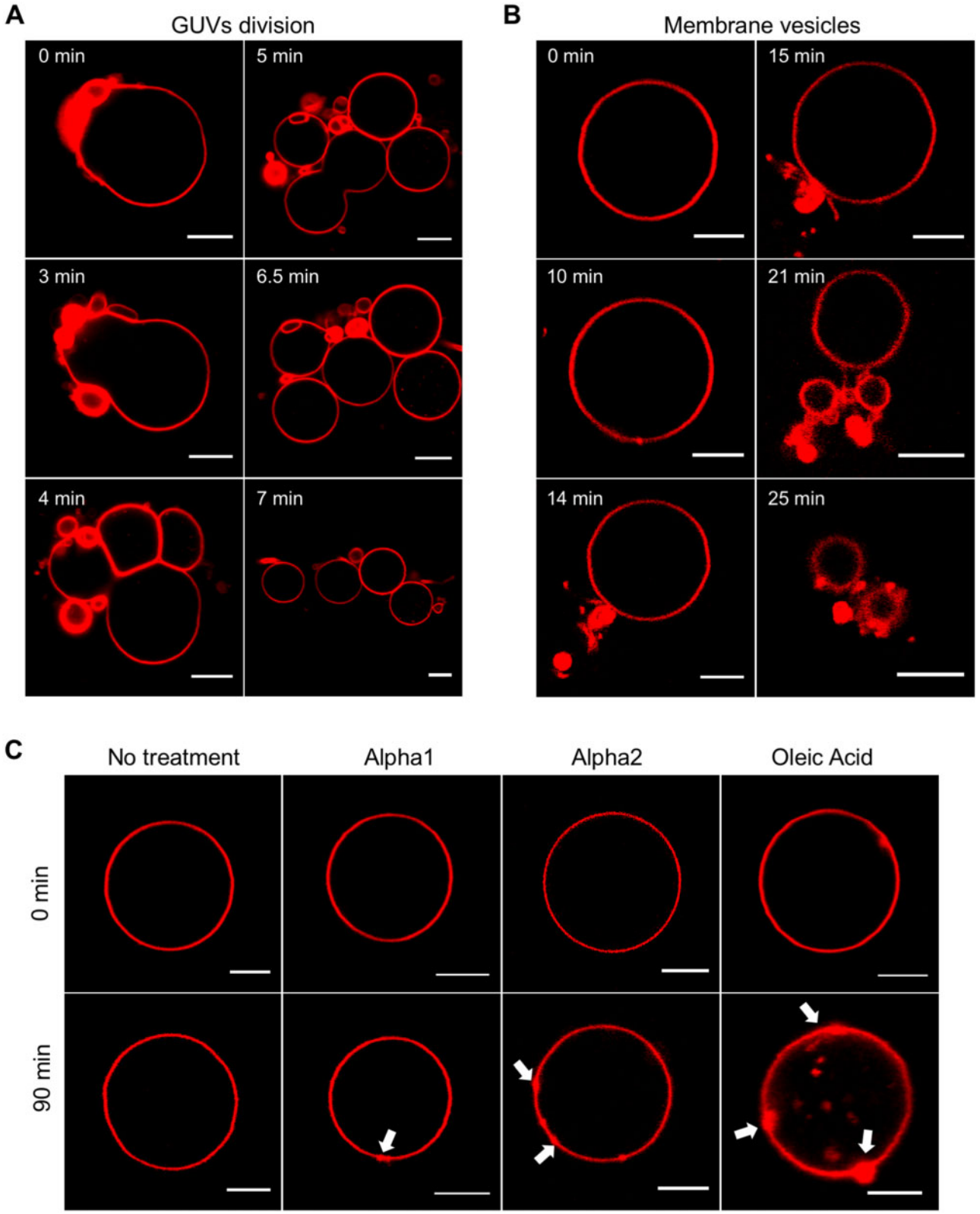

FIG. 1. Alpha-helical peptide–oleate complexes drive the formation of multilumen vesicles. GUVs formed by rhodamine-labeled phosphatidyl choline were exposed to alpha-helical peptide–oleate complexes (21 μM) and monitored in real time by confocal microscopy. (*A*) Alpha2-oleate triggered the formation of a "waist" followed by separation into two halves and division into two or more vesicular entities (8/20, $P < 0.0001$ compared with untreated GUVs, χ^2 test). (*B*) Alpha1-oleate triggered a similar division response with slower kinetics and lower frequency (2/13). In addition, alpha1-oleate triggered the formation of smaller vesicles (13/13, $P = 0.0001$ compared with untreated GUVs, χ^2 test). (*C*) The naked peptides did not drive vesicle division or the formation of smaller vesicles. Lipid redistribution (white arrows) suggested that the peptides affect the membrane structure ($n = 3$). In controls, the GUV morphology remained largely intact for 90 min ($n = 4$).

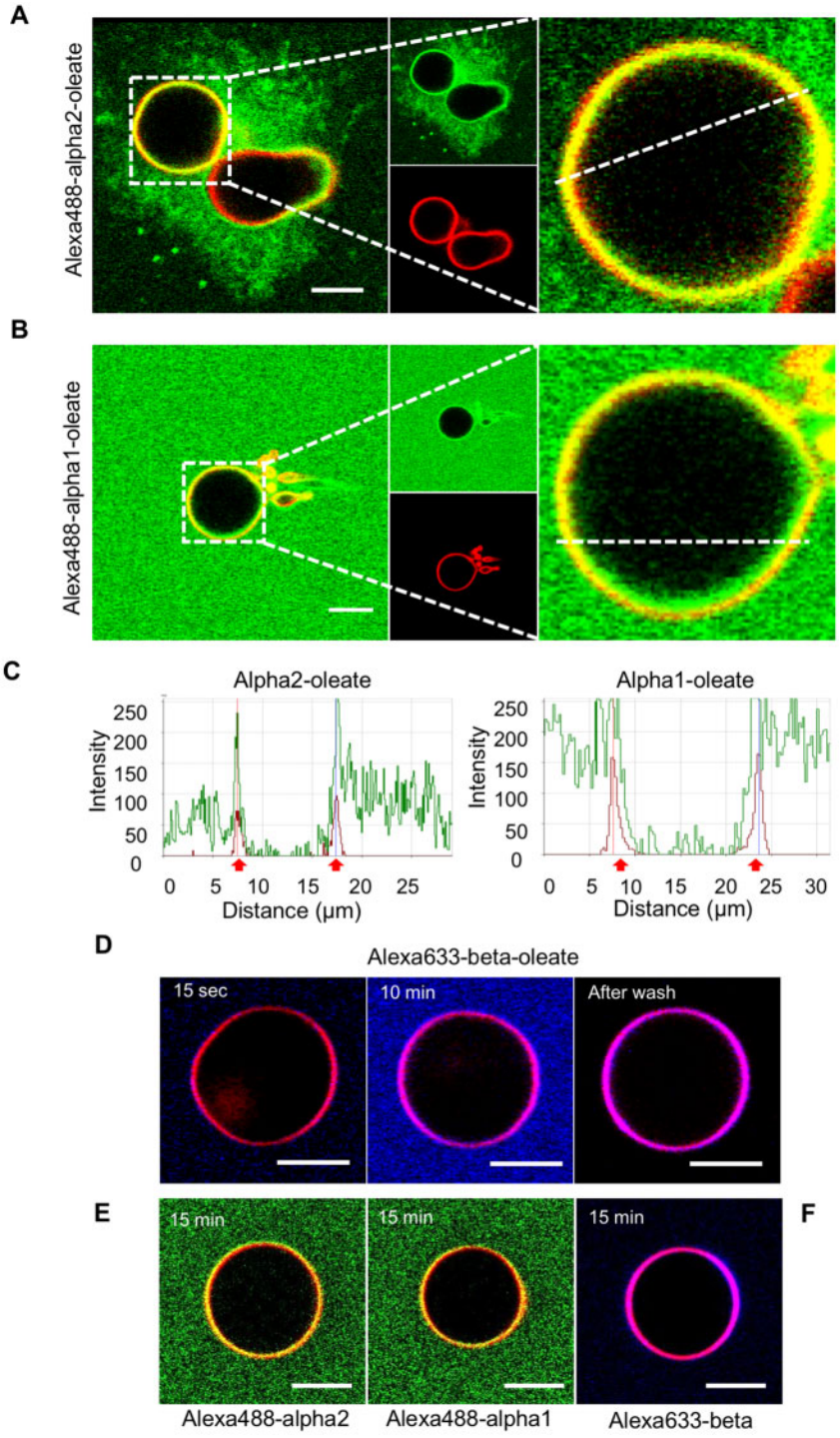

FIG. 2. Colocalization of peptide–oleate complexes with rhodamine-labeled membrane constituents. (*A*, *B*) GUVs formed from rhodamine-labeled phosphatidyl choline (red) were exposed to Alexa 488-labeled alpha2-oleate- or alpha1-oleate complexes (green). Colocalization (yellow) was detected around the vesicle circumference, suggesting membrane insertion of the peptides. (*C*) Colocalization profiles were obtained using the LSM 510 software. Lines in (*A*) and (*B*) indicate the plain of measurement. Arrows indicate significant colocalization. (*D*) Colocalization of beta-oleate complexes (blue) with rhodamine (red) in vesicle membranes (purple). (*E*) Colocalization of Alexa 488-labeled alpha2 and alpha1 peptides (green) with rhodamine (red) in vesicle membranes (yellow). (*F*) Colocalization of Alexa 633-labeled beta peptide (blue) with rhodamine (red) in vesicle membranes (purple).

four GUVs formed smaller membrane vesicles carrying cargo. Continued monitoring detected further GUV division but the fate of the cargo could not be determined at these later time points due to the rapid photobleaching of FITC (fig. 3*C* and *D*).

After exposure to alpha1-oleate, 4/19 GUVs were shown to divide with propagation of cargo (fig. 3*B* and supplementary video 5, Supplementary Material online). In addition, smaller membrane vesicles carrying cargo were observed in six GUVs

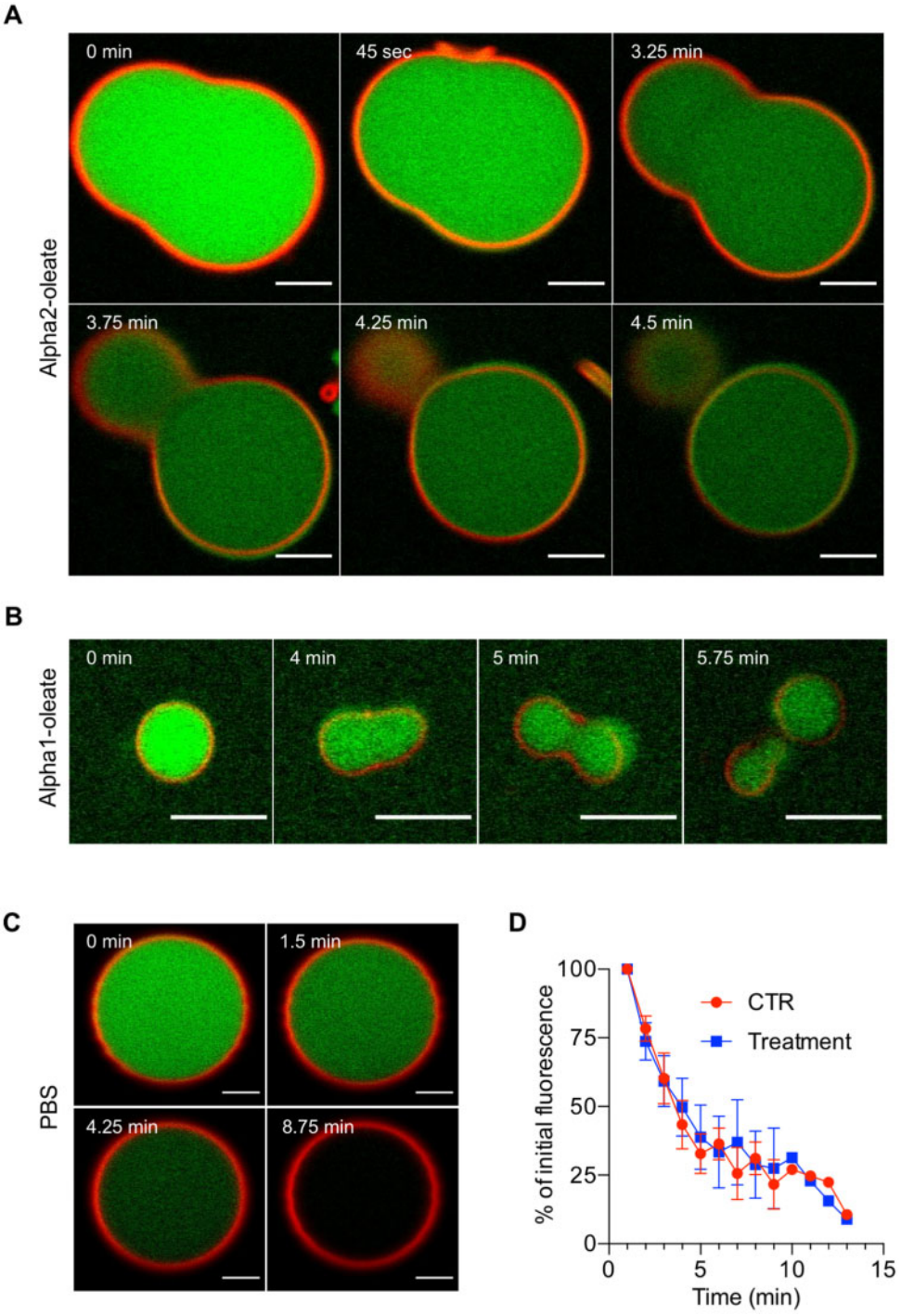

Fig. 3. Coencapsulated cargo is propagated into offspring vesicles. Fluorescein isothiocyanate (FITC)-dextran (green) was incorporated into the GUVs and was retained within the GUVs, as shown by the membrane demarcation (red). (*A*) In response to alpha2-oleate (21 μM), the dextran cargo was efficiently propagated at division into all offspring vesicles. (*B*) In response to alpha1-oleate (21 μM), dextran cargo was also propagated into offspring vesicles. (*C*) Control GUVs in phosphate buffered saline show retention of cargo and a lack of division. (*D*) Photobleaching showed similar kinetics in treated and control vesicles. For statistics, see supplementary table 4, Supplementary Material online.

(supplementary table 4, Supplementary Material online). Control GUVs exposed to phosphate buffered saline (PBS) showed no evidence of division or membrane blebbing (fig. 3C). There was no difference in the kinetics or magnitude of photobleaching between treated and control GUVs, indicating that the macromolecular payloads were retained and not lost to the external environment (fig. 3D).

Lipid Binding of Peptide–Oleate Complexes

The protein lipid overlay assay (Hansen et al. 2017) identifies lipid binding specificities of proteins under nondenaturing solvent conditions (Dowler et al. 2002). To identify lipids targeted by the complexes (fig. 4), Alexa 488-labeled alpha1-oleate and alpha2-oleate or Alexa 633-beta-oleate complexes were examined. Briefly, lipids were spotted onto

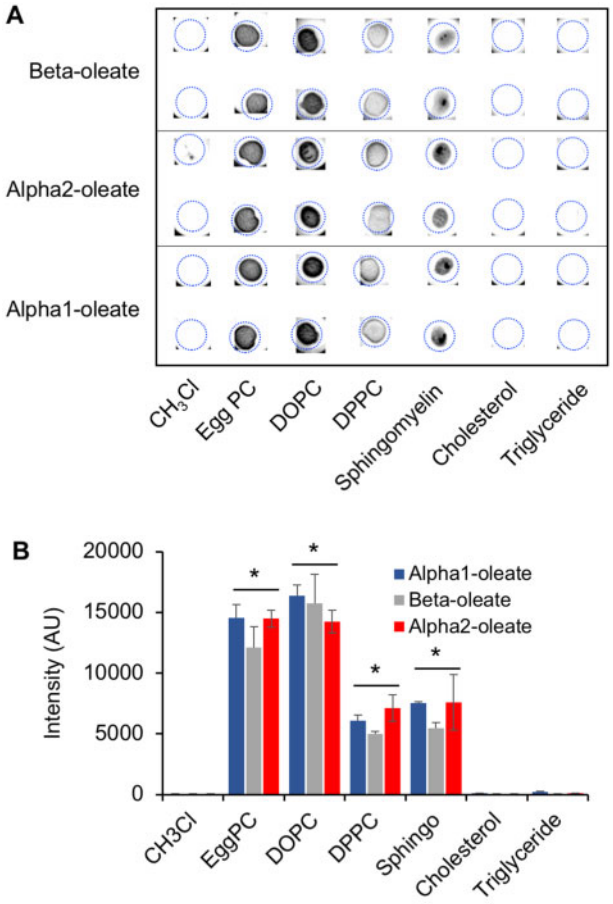

FIG. 4. Lipid binding of peptide–oleate complexes. (*A*) Lipids were spotted in 96-well plates and overlayed with the Alexa 488-alpha1-oleate, Alexa 488-alpha2-oleate, or Alexa 633-beta-oleate complexes. The peptide–oleate complexes were shown to bind DOPC, DPPC, sphingomyelin, and egg PC but not cholesterol or triglycerides. The lipid solvent CH_3Cl was the negative control. (*B*) Quantification of lipid binding in (*A*), mean of four experiments, $^*P < 0.05$ compared with CH_3Cl. Egg PC, egg phosphatidyl choline; DOPC, 1,2-dioleoyl-*sn*-glycero-3-phosphocholine; DPPC, 1,2-dipalmitoyl-*sn*-glycero-3-phosphocholine.

a 96-well plate and binding of each complex was detected by fluorescence imaging (fig. 4*A*). The alpha1- and alpha2-oleate complexes were shown to bind 1,2-dioleoyl-*sn*-glycero-3-phosphocholine, 1,2-dipalmitoyl-*sn*-glycero-3-phosphocholine, or egg phosphatidyl choline but not cholesterol or triglycerides ($P < 0.05$, fig. 4*A* and *B*). In addition, the complexes recognized sphingomyelin, an important membrane constituent involved in cell signaling (Brown and London 2000).

Influence of Peptide Size on Vesicle Division

To address if shorter stretches of amino acids can support vesicle division, we synthesized the N-terminal 15 residues of the alpha1 peptide (alpha1-p1) or residues 10–25 (alpha1-p2) (fig. 5*A*). Alpha1-p1-oleate triggered the formation of membrane blebs and small vesicles (fig. 5*B* and supplementary video 6 and supplementary table 5, Supplementary Material online). In GUVs containing FITC-dextran, two aborted attempts at division were recorded (fig. 5*C*) but most GUVs formed membrane blebs without transfer of cargo (supplementary table 6, Supplementary Material online). Alpha1-p2-oleate caused focal membrane thickening and membrane blebbing but no vesicle formation (fig. 5*B* and supplementary video 7 and supplementary table 5, Supplementary Material online).

The results suggest that a 15 amino acid peptide complex may be sufficient to initiate the membrane response, including the mobilization of cargo, but not to complete vesicle division.

Membrane Effects of Sar1

Sar1 is a member of the Cop II complex that alters membrane curvature and induces tubulation by membrane insertion of its N-terminal amphipathic α-helix (Barlowe et al. 1994; Jensen and Schekman 2011). This N-terminal α-helical domain was synthesized using the yeast sar1 sequence as template (aa 1–23, sar1alpha) (supplementary fig. 1*A*, Supplementary Material online). The sar1alpha peptide was shown to form a complex with oleate and sar1alpha-oleate triggered membrane vesicle formation, tubulation, and membrane blebbing (supplementary fig. 1*B*, supplementary table 7, and supplementary video 8, Supplementary Material online). Using GUVs loaded with FITC-dextran, there was no detectable cargo transfer in response to sar1alpha-oleate, however (supplementary fig. 1*C* and supplementary table 8,

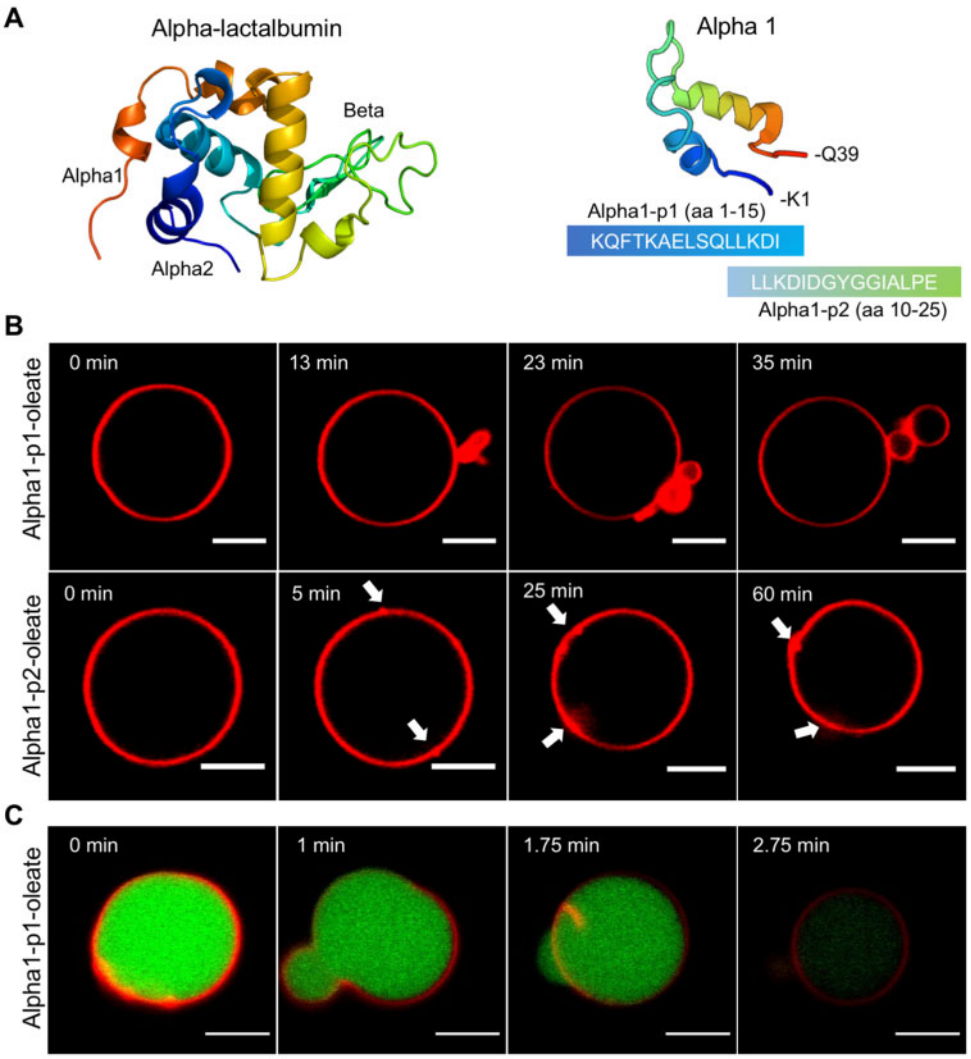

FIG. 5. Membrane effects of shorter peptides derived from alpha1. (*A*) Schematic representation of the alpha-lactalbumin structure (Acharya et al. 1991) indicating the positions of the alpha1, beta and alpha2 domains. Synthetic peptides were derived using alpha1 as a template (alpha1-p1, aa 1–15 or alpha1-p2, aa 10–25). (*B*) Alpha1-p1-oleate induced the formation of small membrane vesicles and blebs (6/6 GUVs) but no vesicle division. Alpha1-p2-oleate caused focal membrane disruptions (white arrows) and blebs (8/17 GUVs) but no GUVs division. (*C*) In dextran-loaded GUVs, alpha1-p1-oleate triggered an incomplete attempt at vesicle division, with initial membrane elongation and waist formation followed by a membrane collapse, returning the vesicle to its spherical shape.

Supplementary Material online) but two aborted attempts at vesicle division were recorded. The shorter N-terminal sar1 peptide (aa 1–15, sar1alpha-p1) triggered the release of membrane blebs (9/9 GUVs, supplementary fig. 1*D*, supplementary video 10, and supplementary table 7, Supplementary Material online).

The results suggest that the N-terminal alpha-helical domain of sar1 does not contain the information necessary to trigger vesicle division and transfer of cargo.

Structural Properties of the Alpha1 and Alpha2 Peptides

The results suggested that the alpha2-oleate complex is a more efficient inducer of GUV division than alpha1-oleate. Structural properties of the peptides and the complexes were compared in an attempt to explain this difference, using pairwise sequence analysis, far-UV circular dichroism spectroscopy, and zeta potential measurement for the naked peptides and the peptide–oleate complexes.

The alpha1 and alpha2 peptides are derived from the N- and C-terminal of human alpha-lactalbumin and are of comparable lengths (39 and 43 residues, respectively) (fig. 6*A* and *B*). Pairwise sequence alignment based on the EMBOSS Needle algorithm showed low identity (2.7%) and similarity (6.8%) (fig. 6*C*). A major difference between the two peptides is the tryptophan content: two in alpha2 and none in alpha1 (fig. 6*A*). Tryptophans play a crucial role in anchoring peptides and proteins to membrane interfaces (de Jesus and Allen 2013) due to the highest molecular mass (186 g/mol), largest volume (237.6 $Å^3$), largest free surface area (255 $Å^2$) available for contact with spherical molecules like water bound to membrane surfaces, and the highest hydrophobicity index in both octanol and interfacial scales (Chothia 1975, 1976; Richards 1977; Wimley and White 1996; Wimley et al. 1996). Important

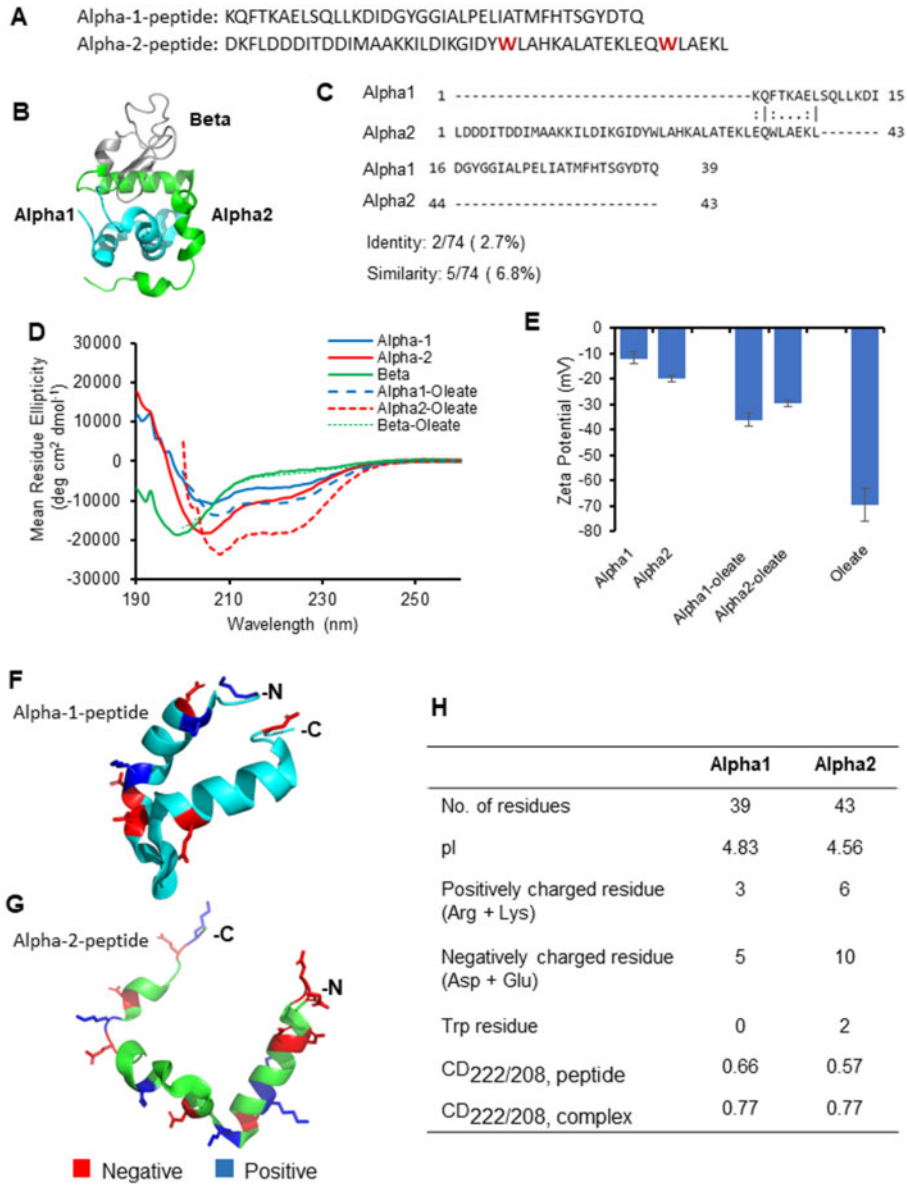

FIG. 6. Sequence and structural analysis of alpha1 and alpha2 peptides. (*A*) Sequences of the alpha1 and alpha2 peptides with the tryptophans highlighted. (*B*) Schematic representation of human alpha-lactalbumin (PDB: 1HML). Alpha1 and alpha2 sequences are highlighted in cyan and green, respectively. The beta sequence is in gray. (*C*) Pairwise sequence alignment of alpha1 and alpha2 using EMBOSS Needle algorithm. (*D*) Far-UV circular dichroism spectra of the peptides and peptide–oleate complexes. (*E*) Zeta potential measurement for the peptides and peptide–oleate complexes. (*F*, *G*) Schematic representation of alpha1 and alpha2 structures highlighting charged amino acid residues (PDB: 1HML). (*H*) Table summarizing the biophysical properties of the alpha1 and alpha2 peptides.

enthalpic factors that facilitate membrane interactions include electrostatic forces such as pi–pi and cation–pi interactions; hydrogen bonding ability and dipolar interactions with membrane lipids (Esbjorner et al. 2007; Sun et al. 2008; Blaser et al. 2009). Entropic factors include interactions with lipid and bilayer structures, as well as the hydrophobic effect (White and Wimley 1999; McIntosh et al. 2001). The presence of two tryptophan residues in alpha2 peptides is predicted to increase the anchoring to zwitterionic membranes potentially resulting in more efficient delivery of an oleic acid load to the membrane.

Far-UV circular dichroism spectra and secondary structure predictions further revealed high helical content in the naked and oleate-bound peptides (~90%) (fig. 6*D*). Upon peptide–oleate complex formation, alpha1 and alpha2 both showed enhanced alpha-helicity and similar 222/208 ratios (Kelly and Price 1997). Therefore, despite the lack of sequence homology, the structural features of the two peptides appear to be similar (fig. 6*D*). However, the number of charged residues was higher in the alpha2 sequence than in alpha1 as predicted from the full-length human alpha-lactalbumin structure (PBD: 1HML). The even distribution of charged residues along the alpha2 sequence may effectively contribute to the observed membrane remodeling activity. The difference in overall charge between the alpha1 and alpha2 peptides was confirmed by zeta potential measurements (fig. 1*E*). The relatively low zeta potential of alpha2-oleate indicates that

charged residues may be involved in the entrapment of oleate residues within the complex (Xie et al. 2013).

Discussion

Protocell division is critically important for early life propagation. Identifying the minimal machinery involved in this division has been quite challenging, however (Mizushina et al. 1997; Jin et al. 2018). Intriguingly, to our knowledge, no single molecular species has been reported to drive protocell division and for peptides, no plausible mechanism has been identified (Murtas 2013). In this study, we made the surprising observation that complexes formed by short alpha-helical peptides and oleic acid become integrated into lipid bilayers and drive the formation of novel, membrane-enclosed entities from a single lipid vesicle. This membrane response did not require cofactors or an external energy source, suggesting that peptide–oleate complexes contain the molecular information necessary to initiate and sustain this process. The effect was specific for alpha-helical peptide–oleate complexes, as naked peptides were inactive and oleic acid alone caused internal tubulation but no membrane blebbing. The results suggest a simple model to understand how fatty acid/phospholipid intermediates can drive protocell division, aided by a small peptide capable of membrane integration and oleic acid binding.

Oleic acid has been extensively used to model protocells and to study how membranes evolve through a hybrid fatty acid/phospholipid state to the phospholipid bilayers that now define cells in complex tissues (Schrum et al. 2010; Budin and Szostak 2011; Budin et al. 2014; Exterkate et al. 2018). It is known that certain environmental chemicals promote vesicle growth (Zhu et al. 2012; Tang et al. 2014) and peptides have been suggested to drive this process, as their synthesis has been demonstrated to occur under assumed early life conditions, such as hydrothermal vents (White et al. 1984). Short polypeptide sequences or structural motifs existed in the prebiotic world and intriguingly the incorporation of dipeptide catalysts into fatty acid membranes enhances the expansion of the lipid vesicles (Adamala and Szostak 2013). Although the 45-kDa bacterial FtsZ protein, a homolog of tubulin that hydrolyzes guanosine triphosphate (Erickson 2007), has been suggested as progenitor for a mode of early life protocell division, it has not been shown to drive protocell cell division on its own (Du et al. 2018). Therefore, its role has so far been difficult to place in the origin of protocell division.

Although peptides and oleic acid separately engaged the vesicular membranes, each constituent alone did not trigger blebbing or vesicle division, suggesting that the complex needs to be formed, prior to membrane contact. We speculate that as oleic acid partitions into the lipid bilayer, as is seen under conditions of vesicle growth. Importantly, a large number of interacting residues remained available after complex formation, indicating that the binding of oleic acid does not hinder membrane interactions of lipid binding peptide residues (Chaudhuri et al. 2016). Lipid interactions with the peptides were detected here using a dot blot assay, and although binding partners included phospholipids, evolved membrane constituents such as cholesterol were not recognized. The gradual accumulation of the peptide–oleate complex would be predicted to extend the membrane, disturbing the balanced, spherical form of the vesicle and triggering membrane reorganization, resulting in the active formation of membrane blebs and new vesicular entities.

The fate of the oleic acid load of the complex and its partitioning into the membranes merits comment. Monitoring the fate of oleic acid upon binding of the complex to membranes is a challenging task even with high-resolution microscopy. We therefore performed an exhaustive computational study using coarse-grained molecular dynamics simulations to monitor the binding of bovine alpha-lactalbumin complex to zwitterionic and negatively charged membranes (Chaudhuri et al. 2016). We recently observed unloading and partitioning of oleic acid into the outer leaflet of the membrane and then flip-flop movement into the inner leaflet of the bilayer consisting of negatively charged and zwitterionic lipids (unpublished data). We speculate that the asymmetry in oleic acid partitioning is initiated by deposition of peptide bound oleic acid into the outer leaflet, resulting in curvature stress at initiation sites of cleavage or membrane fission.

The lysozyme gene is 400–600 My old and lysozyme is an essential enzyme for the defense of all life in general, placing this family of proteins in an early evolutionary context. It may be speculated that the peptides used here represent early stages of protein evolution, before the sophistication of higher organisms required proteins to adopt stable three-dimensional conformations and domain structures. Alpha-lactalbumin arose from lysozyme after a series of gene duplications (300–400 Ma) (Prager and Wilson 1988) and the N- and C-terminal alpha-lactalbumin peptides retain detectable alpha-helical structure but are partially unfolded, possibly reflecting a structurally more primitive state that defines their ability to bind oleic acid and form complexes (Mok et al. 2005). The evolved chimeric structure of α-lactalbumin in mammals may reflect the need to solve emergent challenges during evolution. Deduced from its role in protocell division, alpha2 might be the most ancient domain. The beta-sheet domain binds heat shock proteins, which target the complex to the lysosomes, potentially equipping the protein with a mechanism to limit the extent of cell division (Nadeem et al. 2019). Finally, the alpha1 domain, which disrupts membrane integrity in immature cells, may serve to drive differentiation, by favoring the survival of cells with a more evolved membrane structure. This domain is exposed in partially unfolded alpha-lactalbumin and the affinity for oleate creates an alpha1-oleate complex with broad anticancer activity (Ho et al. 2013). All in one protein—kind of cool!

Materials and Methods

Peptides

Peptides were synthesized using Fmoc solid phase chemistry (Mimotopes, Australia) and purity defined by mass spectrometry (supplementary table 1, Supplementary Material online).

Preparation of GUVs

GUVs were formed by hydrogel-assisted swelling according to established protocols (Horger et al. 2009; Hansen et al. 2013), with modifications previously described (Peruzzi et al. 2016). Briefly, glass cover slips were sonicated in 1 M NaOH solution (30 min), rinsed in Milli-Q water (3×), and further sonicated (30 min). Coverslips were plasma etched (1 min) using a BD-20 laboratory corona treater (Electro Technic Products Inc., USA) to render the surface clean and hydrophilic. A thin film of 1% (w/v) solution of molten ultra-low gelling temperature type IX-A agarose (Sigma-Aldrich, USA) was deposited on the coverslip to provide a reaction bed for GUV formation. The cover slips were placed in AttoFluor cell chambers (Thermo Fisher Scientific, USA). Following, 10 μl of egg phosphatidyl choline (Avanti Polar Lipids, USA) in chloroform (25 mg/ml) doped with 4% v/v rhodamine C (1 mg/ml, Sigma-Aldrich) were deposited onto the gelled agarose surface to enable visualization and the solvent evaporated with nitrogen gas. The lipid-hydrogel film was rehydrated with 200 mM sucrose in PBS, pH 7.2 for 25 min before gentle aspiration using wide-bore pipette tips and transfer into 200 mM glucose in PBS, pH 7.2 for sedimentation. GUVs were allowed to settle for 30 min before visualization.

Encapsulation of FITC-Dextran Macromolecules

For the incorporation of macromolecules, GUVs were formed by hydrogel-assisted swelling with egg phosphatidyl choline and 1,2-dioleoyl-*sn*-glycero-3-phosphoethanolamine (Avanti Polar Lipids) in a 1:1 molar ratio. Fluorescein isothiocyanate (FITC)-dextran (FD4, Sigma-Aldrich) was dissolved into the sucrose buffer at a 100 μM working solution, and the lipid-hydrogel film was rehydrated following the same procedure described above (Hansen et al. 2011).

Complex Preparation and Treatment

Peptide–oleate complexes were prepared as previously described (Brisuda A, Ho J, Kandiyal P, Ng J, Ambite I, Butler D, Háček J, Tran TH, Wan MLY, Hastings A, Tran TH, Fortunati D, Storm P, Nadeem A, Novotna H, Horňák J, Hansen JS, Mu YG, Mok KH, Babjuk M, Svanborg C, unpublished data). Briefly, each peptide was dissolved in PBS (pH 7.2) and oleic acid was added at five times molar excess. For imaging, the peptides were labeled with Alexa Fluor 488 (alpha1 and alpha2 peptides) or Alexa Fluor 633 (beta peptide) (Thermo Fisher Scientific).

Real-Time Confocal Imaging

Alexa-labeled complexes or peptides were added to the GUVs in chamber (8 chamber, Lab-Tek II chambered #1.5 German coverglass system, Thermo Fisher Scientific) and membrane changes were visualized by real-time confocal microscopy (21 μM, 20% labeled peptide). The GUVs were washed by gentle rinse using 200 mM glucose solution. Images were acquired on a Zeiss LSM 510 META confocal laser-scanning microscope and background corrected using the in-built ImageJ rolling-ball filter (Abràmoff et al. 2004). Upon complex treatment, the GUVs started to move which resulted in the shift between images of the two different channels. For the correction, the offset of two channels was realigned using Image.

Protein Lipid Overlay Assay

The affinity for phospholipids and sterols was investigated using a lipid overlay assay (Dowler et al. 2002). Lipids dissolved in chloroform (25 mg/ml) were added to individual wells in a 96-well plate (1 µl/well, supplementary table 2, Supplementary Material online). After drying (2 h), Alexa-labeled peptide–oleate complexes or peptides were added (30 µM), incubated for 1 h and washed with PBS-Tween 20 (100 µl, 0.1%). The signal was captured using a ChemiDoc XRS+ System (BioRad, USA).

Statistical Analysis

All statistical analysis is calculated using Prism 6 software (GraphPad, USA). Tests with categorical variables including GUV division, membrane vesicles, and blebs were performed by Pearson's χ^2 test. For the comparison of binding between peptide–oleate complexes and different lipids, data were analyzed by Mann–Whitney *U* test. Statistical significance was considered with $P < 0.05$.

Supplementary Material

Supplementary data are available at *Molecular Biology and Evolution* online.

Acknowledgments

This study was supported by grants from the Swedish Cancer Society, the Medical Research Council, the Swedish Research Council (#2016-01952, #2019-01196), European Union's Horizon 2020 research and innovation programme (EIC Accelerator), grant agreement no. 954360 Hamlet-BC, Faculty of Lund University, Söderberg Foundation, Maggie Stephens Foundation, Österlund Foundation, Inga-Britt and Arne Lundberg Foundation, and H.J. Forssman Foundation for Medical Research and Royal Physiographic Society. The study was also supported by a grant from Hamlet Pharma to Lund University.

References

Abràmoff MD, Magalhães PJ, Ram SJ. 2004. Image processing with ImageJ. *Biophotonics Int.* 11:36–42.

Acharya KR, Ren J, Stuart DI, Phillips DC, Fenna RE. 1991. Crystal structure of human α-lactalbumin at 1.7 Å resolution. *J Mol Biol.* 221(2):571–581.

Adamala K, Szostak JW. 2013. Competition between model protocells driven by an encapsulated catalyst. *Nat Chem.* 5(6):495–501.

Aminlari L, Hashemi MM, Aminlari M. 2014. Modified lysozymes as novel broad spectrum natural antimicrobial agents in foods. *J Food Sci.* 79(6):R1077–R1090.

Barlowe C, Orci L, Yeung T, Hosobuchi M, Hamamoto S, Salama N, Rexach MF, Ravazzola M, Amherdt M, Schekman R. 1994. COPII: a membrane coat formed by Sec proteins that drive vesicle budding from the endoplasmic reticulum. *Cell* 77(6):895–907.

Blaser G, Sanderson JM, Wilson MR. 2009. Free-energy relationships for the interactions of tryptophan with phosphocholines. *Org Biomol Chem.* 7(24):5119–5128.

Brown DA, London E. 2000. Structure and function of sphingolipid- and cholesterol-rich membrane rafts. *J Biol Chem.* 275(23):17221–17224.

Budin I, Bruckner RJ, Szostak JW. 2009. Formation of protocell-like vesicles in a thermal diffusion column. *J Am Chem Soc*. 131(28):9628–9629.
Budin I, Debnath A, Szostak JW. 2012. Concentration-driven growth of model protocell membranes. *J Am Chem Soc*. 134(51):20812–20819.
Budin I, Prywes N, Zhang N, Szostak JW. 2014. Chain-length heterogeneity allows for the assembly of fatty acid vesicles in dilute solutions. *Biophys J*. 107(7):1582–1590.
Budin I, Szostak JW. 2011. Physical effects underlying the transition from primitive to modern cell membranes. *Proc Natl Acad Sci U S A*. 108(13):5249–5254.
Chaudhuri A, Prasanna X, Agiru P, Chakraborty H, Rydström A, Ho JC, Svanborg C, Sengupta D, Chattopadhyay A. 2016. Protein-dependent membrane interaction of a partially disordered protein complex with oleic acid: implications for cancer lipidomics. *Sci Rep*. 6(1):35015.
Chothia C. 1975. Structural invariants in protein folding. *Nature* 254(5498):304–308.
Chothia C. 1976. The nature of the accessible and buried surfaces in proteins. *J Mol Biol*. 105(1):1–12.
de Jesus AJ, Allen TW. 2013. The role of tryptophan side chains in membrane protein anchoring and hydrophobic mismatch. *Biochim Biophys Acta* 1828(2):864–876.
Dominak LM, Keating CD. 2007. Polymer encapsulation within giant lipid vesicles. *Langmuir* 23(13):7148–7154.
Dowler S, Kular G, Alessi DR. 2002. Protein lipid overlay assay. *Sci STKE* 2002(129):pl6.
Du S, Pichoff S, Kruse K, Lutkenhaus J. 2018. FtsZ filaments have the opposite kinetic polarity of microtubules. *Proc Natl Acad Sci U S A*. 115(42):10768–10773.
Erickson HP. 2007. Evolution of the cytoskeleton. *BioEssays* 29(7):668–677.
Esbjorner EK, Caesar CE, Albinsson B, Lincoln P, Norden B. 2007. Tryptophan orientation in model lipid membranes. *Biochem Biophys Res Commun*. 361(3):645–650.
Exterkate M, Caforio A, Stuart MC, Driessen AJ. 2018. Growing membranes in vitro by continuous phospholipid biosynthesis from free fatty acids. *ACS Synth Biol*. 7(1):153–165.
Fanti A, Gammuto L, Mavelli F, Stano P, Marangoni R. 2018. Do protocells preferentially retain macromolecular solutes upon division/fragmentation? A study based on the extrusion of POPC giant vesicles. *Integr Biol*. 10(1):6–17.
Hansen JS, de Mare S, Jones HA, Goransson O, Lindkvist-Petersson K. 2017. Visualization of lipid directed dynamics of perilipin 1 in human primary adipocytes. *Sci Rep*. 7(1):15011.
Hansen JS, Thompson JR, Hélix-Nielsen C, Malmstadt N. 2013. Lipid directed intrinsic membrane protein segregation. *J Am Chem Soc*. 135(46):17294–17297.
Hansen JS, Vararattanavech A, Vissing T, Torres J, Emnéus J, Hélix-Nielsen C. 2011. Formation of giant protein vesicles by a lipid cosolvent method. *ChemBioChem* 12(18):2856–2862.
Helfrich MR, Mangeney-Slavin LK, Long MS, Djoko KY, Keating CD. 2002. Aqueous phase separation in giant vesicles. *J Am Chem Soc*. 124(45):13374–13375.
Ho JC, Storm P, Rydström A, Bowen B, Alsin F, Sullivan L, Ambite I, Mok KH, Northen T, Svanborg C. 2013. Lipids as tumoricidal components of human α-lactalbumin made lethal to tumor cells (HAMLET): unique and shared effects on signaling and death. *J Biol Chem*. 288(24):17460–17471.
Horger KS, Estes DJ, Capone R, Mayer M. 2009. Films of agarose enable rapid formation of giant liposomes in solutions of physiologic ionic strength. *J Am Chem Soc*. 131(5):1810–1819.
Jensen D, Schekman R. 2011. COPII-mediated vesicle formation at a glance. *J Cell Sci*. 124(1):1–4.
Jin L, Kamat NP, Jena S, Szostak JW. 2018. Fatty acid/phospholipid blended membranes: a potential intermediate state in protocellular evolution. *Small* 14(15):1704077.
Kelly SM, Price NC. 1997. The application of circular dichroism to studies of protein folding and unfolding. *Biochim Biophys Acta* 1338(2):161–185.
Lancet D, Zidovetzki R, Markovitch O. 2018. Systems protobiology: origin of life in lipid catalytic networks. *J R Soc Interface* 15(144):20180159.
McIntosh TJ, Vidal A, Simon SA. 2001. The energetics of binding of a signal peptide to lipid bilayers: the role of bilayer properties. *Biochem Soc Trans*. 29(4):594–598.
Mizushina Y, Yoshida S, Matsukage A, Sakaguchi K. 1997. The inhibitory action of fatty acids on DNA polymerase β. *Biochim Biophys Acta Gen Subj*. 1336(3):509–521.
Mok KH, Nagashima T, Day IJ, Hore P, Dobson CM. 2005. Multiple subsets of side-chain packing in partially folded states of α-lactalbumins. *Proc Natl Acad Sci U S A*. 102(25):8899–8904.
Murtas G. 2013. Early self-reproduction, the emergence of division mechanisms in protocells. *Mol Biosyst*. 9(2):195–204.
Nadeem A, Ho JC, Tran TH, Paul S, Granqvist V, Despretz N, Svanborg C. 2019. Beta-sheet-specific interactions with heat shock proteins define a mechanism of delayed tumor cell death in response to HAMLET. *J Mol Biol*. 431(14):2612–2627.
Nadeem A, Sanborn J, Gettel DL, James HCS, Rydström A, Ngassam VN, Klausen TK, Pedersen SF, Lam M, Parikh AN, et al. 2015. Protein receptor-independent plasma membrane remodeling by HAMLET: a tumoricidal protein-lipid complex. *Sci Rep*. 5:16432.
Peruzzi J, Gutierrez MG, Mansfield K, Malmstadt N. 2016. Dynamics of hydrogel-assisted giant unilamellar vesicle formation from unsaturated lipid systems. *Langmuir* 32(48):12702–12709.
Prager EM, Wilson AC. 1988. Ancient origin of lactalbumin from lysozyme: analysis of DNA and amino acid sequences. *J Mol Evol*. 27(4):326–335.
Richards FM. 1977. Areas, volumes, packing and protein structure. *Annu Rev Biophys Bioeng*. 6(1):151–176.
Schrum JP, Zhu TF, Szostak JW. 2010. The origins of cellular life. *Cold Spring Harb Perspect Biol*. 2(9):a002212.
Spector AA, Yorek MA. 1985. Membrane lipid composition and cellular function. *J Lipid Res*. 26(9):1015–1035.
Sun H, Greathouse DV, Andersen OS, Koeppe RE 2nd. 2008. The preference of tryptophan for membrane interfaces: insights from *N*-methylation of tryptophans in gramicidin channels. *J Biol Chem*. 283(32):22233–22243.
Tang TD, Hak CRC, Thompson AJ, Kuimova MK, Williams D, Perriman AW, Mann S. 2014. Fatty acid membrane assembly on coacervate microdroplets as a step towards a hybrid protocell model. *Nat Chem*. 6(6):527–533.
White DH, Kennedy RM, Macklin J. 1984. Acyl silicates and acyl aluminates as activated intermediates in peptide formation on clays. *Origins Life Evol Biosph*. 14(1–4):273–278.
White SH, Wimley WC. 1999. Membrane protein folding and stability: physical principles. *Annu Rev Biophys Biomol Struct*. 28(1):319–365.
Wimley WC, Creamer TP, White SH. 1996. Solvation energies of amino acid side chains and backbone in a family of host–guest pentapeptides. *Biochemistry* 35(16):5109–5124.
Wimley WC, White SH. 1996. Experimentally determined hydrophobicity scale for proteins at membrane interfaces. *Nat Struct Mol Biol*. 3(10):842–848.
Xie Y, Min S, Harte NP, Kirk H, O'Brien JE, Voorheis HP, Svanborg C, Hun Mok K. 2013. Electrostatic interactions play an essential role in the binding of oleic acid with alpha-lactalbumin in the HAMLET-like complex: a study using charge-specific chemical modifications. *Proteins* 81(1):1–17.
Zhu TF, Adamala K, Zhang N, Szostak JW. 2012. Photochemically driven redox chemistry induces protocell membrane pearling and division. *Proc Natl Acad Sci U S A*. 109(25):9828–9832.